J Indian Inst Sci., Sept.–Oct. 1996, **76**, 589–602
© Indian Institute of Science

Optical phase conjugation by degenerate four-wave mixing in tetraphenylporphines

B. RAGHAVENDRA PRASAD AND C. K. SUBRAMANIAN
Department of Physics, Indian Institute of Science, Bangalore 560 012, India.

Received on January 27, 1995; Revised on December 20, 1995.

Abstract

Systematic and detailed studies of thermally induced degenerate four-wave mixing (DFWM) in metal-substituted tetraphenylporphines and four different solvents have been carried out to understand the physics of the process and to optimize the parameters for maximum efficiency. These studies include the effect of the angle of interaction and coherence length, the roles played by different solvent parameters, the absorption coefficients and the quantum efficiencies of different dye–solvent combinations, the effect of reverse saturable absorption on the efficiency of the system, the intensity dependence, the wavelength dependence and finally the phase conjugate nature of the signal

Keywords: Phase conjugation, four-wave mixing, thermal gratings, tetraphenylporphines

1. Introduction

Degenerate four-wave mixing (DFWM) in nonlinear optics refers to the process in which three input optical waves of the same frequency interact in a medium and generate a fourth wave of identical frequency. Such processes are allowed in all media. In this process, two of the three input waves can beat and drive the material excitations. The process is nonresonant in general and a particular material excitation will dominate only if it happens to be resonantly driven. In any case, the material excitational wave can mix with the third input wave to yield a nonlinear polarization at the resonant beat frequency; the latter then generates and radiates the coherent output. In the above picture, the material excitational wave can also be regarded as a moving grating or dynamic grating in the medium. The coherent output is then the result of diffraction of the third input wave from the moving grating. A particular material excitation may dominate in the grating formation if it is resonantly excited.

The generation of phase conjugate signals by the technique of formation of thermal gratings in absorbing media, especially of dye solutions, has been shown to have several advantages. The underlying physical phenomenon involves the generation of density and temperature fluctuations following the absorption of light through electronic transitions in the absorbing molecules and the subsequent thermalization through radiationless relaxation of the optically excited molecules causing local heating. This gives rise to periodic temperature (or entropy) fluctuations in some cases and density fluctuations in others. These result in a spatial modulation of the refractive index of the solvent which then acts as a phase grating in the scattering of the incident light. The physics of the process and the outline of the theoretical model followed are discussed here.

2. Theory

Various theoretical models have been proposed to account for the optically induced thermal fluctuations in an absorbing medium. Most important among these are the hydrodynamic model and the heat-diffusion model. The hydrodynamic model takes into account the transient nature of the process, including the effects of non-negligible thermalization rise time on the grating formation dynamics coupled with contributions due to density changes resulting from thermal expansion of compressible media. The coupled hydrodynamic-electromagnetic theory includes the full-time dependence of the grating evolution as well as the initial effects of acoustic modes and thermalization effects. The first theoretical model for stimulated scattering of light was proposed by Bathra *et al.*[1] Hoffman[2] based her investigations on this approach and extended it to thermally induced DFWM. In Hoffman's approach, the dynamics of the thermal grating formation is modelled in terms of a set of three coupled hydrodynamic equations describing the behavior of the medium in the presence of appropriate nonlinear polarization.

The full hydrodynamic theory of formation of thermal gratings, and their subsequent effect on the incident electric fields creating the gratings, is not analytically tractable[2]. Several simplifying assumptions have to be made to provide analytical solutions that, however, contain all the physics of the temporal formation of the grating and its effect on a scattered electromagnetic wave. It is assumed that the incident electric fields deplete only by absorption in the media (small-signal approximation)[3,4]. This implies that the 'small' effect of the grating on the transverse structure in the amplitudes of the incident fields can be neglected. Thus the incident fields effectively act to produce a harmonic grating in the medium whose time dependence is determined only by the hydrodynamics of the complete absorption process. It is also assumed that the grating dynamics are determined by the first-order changes in the liquid dielectric constant. These changes are due to the absorption of energy from the incident electric fields, and are pure harmonic in the grating wave vector, leading to a periodic grating whose strength changes with time, but with a shape that is time independent. Thus a separation of the writing and reading process is effected leading to a tractable solution.

A detailed analysis assuming that the slowly varying amplitudes of the thermodynamic quantities then give an expression for the phase conjugate reflectivity. By assuming rectangular pulse shapes for the electric field amplitudes, an approximate analytical expression for the reflectivity R is finally obtained as[2]

$$R = f^2 Q^2 e^{-\alpha L \sec\theta}\left(1-e^{-\alpha L}\right)^2 I_1 I_2 G(t_D) \tag{1}$$

where

$$Q = \frac{2n(dn/dT)_p}{\lambda \rho_0 C_p} \tag{2}$$

$$G(t_D) = \frac{1}{\tau_{eff}^2 t'_p} \int^{t_D + t'_p} dt F^2(t,T) \tag{3}$$

and

$$F(t,T)=\frac{1}{\Gamma_u}\int_0^T dt'\left[1-\exp(-\Gamma_u t')\right]\left[\exp\left[\frac{-\left(t_p-t'_p\right)}{\tau_R}\right]-\exp\left[-\frac{\Gamma_B(t-t')}{2}\right]\cos\omega_B(t-t')\right] \quad (4)$$

In eqn (1), I_1 and I_2 are the pump and read beam intensities, f, the phenomenological factor defined as the fraction of the absorbed light energy converted into heat[5,6]. In eqn (4), $1/\Gamma_u$ is the thermalization time due to non-instantaneous and nonlocal solute–solvent energy transfer, Γ_B, the full Brillouin linewidth, t_p and t'_p are, respectively, the probe and phase conjugate pulse durations, ω_B is the Brillouin frequency and τ_R, the Rayleigh lifetime or thermal grating decay time.

The term $G(t_D)$ given in eqn (3) contains details of thermal grating build-up and decay where t_D represents the time delay of the backward-propagating 'read' beam with respect to the forward-propagating pump and probe beams. An approximate expression of $G(t_D)$, for a short time delay region, *i.e.*, $t_D << t_p - t'_p$, is given as[7,8]

$$G(t_D)\approx\frac{t_p'^2}{3\tau_{eff}^2\Gamma_u^2}\left[1+\frac{3t_D\left(t_D+t'_p\right)}{t_p'^2}\right] \quad (5)$$

and

$$\tau_{eff}\Gamma_u=1+\tau_{eff}Dq^2 \quad (6)$$

where τ_{eff} is the effective thermalization time, D, the diffusion time constant of the solute–solvent, and q, the thermal grating wave vector given by $q = 2\mathrm{k}\sin(\theta/2)$ where $k = n\omega/\mathrm{c}$, θ, the angle of interaction and ω, the frequency of the incident electromagnetic field.

In the hydrodynamic model discussed above, there is no explicit representation of the third-order nonlinear susceptibility $\chi^{(3)}$ which determines the optical phase conjugate (OPC)–DFWM efficiency of the solute–solvent system. All the physical and laser parameters that govern the efficiency of the system are contained in eqn (1) for the phase conjugate reflectivity. The magnitude of $\chi^{(3)}$ is determined by the expression given by Caro and Gower[9], and it may have contributions from several nonlinear processes such as thermal, orientational and population-grating effects[10].

$$\chi^{(3)}=\frac{4c^2n^2\varepsilon_0\alpha}{3\omega e^{-\alpha L\sec\theta}\left[1-e^{-\alpha L}\right]}\frac{\sqrt{R}}{I} \quad (7)$$

and for pure thermal gratings[9]

$$\chi^{(3)}=\frac{dn}{dT}\left[\frac{4n^2c\varepsilon_0\tau\alpha\phi}{3\rho C_p}\right] \quad (8)$$

where τ is the pulse duration, α, the absorption coefficient, n, the refractive index, ρ, the density, C_p, the specific heat, dn/dT, the change in the refractive index with temperature and ϕ, the fraction of the absorbed energy converted into heat.

The simplified expressions given above are rendered valid by a careful choice of parameters in accordance with the conditions prevailing in the specific experimental situations of interest. All the time scales that are involved can be classified as those that characterize the medium and those that characterize the laser parameters. Information regarding thermal grating formation and decay can be predicted by the relationships between them. In this theory, a simple model for the energy levels of the solute is assumed. Complex time-dependent effects of fluorescence have been ignored. These introduce some uncertainty in the exact determination of the diffusion constant and thermalization time. Most of the absorbing molecules cannot be represented by a simple two-level systems. A more complete description of the solute–solvent interaction has to consider details of the contributions due to rotational, vibrational and electronic nonradiative relaxation and also the long-lived excited state decay. The inclusion of these parameters also depends on the solute under consideration. All these mechanisms play an important role when integrated reflectivities are deduced as a function of read beam time delay.

For optimal thermal grating efficiencies a careful choice of the laser and medium time scales have to be made as is evident from the theory outlined above. The influence of solvent–dye combinations, geometrical arrangements, read beam time delays, laser pulse durations, angle of interaction between the pump and probe beams, coherence length of the laser, proper concentration–interaction length product for the chosen dye system, the system geometry and optimum beam intensities to avoid saturation and spurious scattering effects must be considered carefully for higher phase conjugate reflectivities. A systematic study of thermally induced DFWM in dye solutions has therefore been taken up here.

3. Experimental

The experimental layout is shown in Fig. 1. The experiments are conducted using the second harmonic of the Nd:YAG laser, *i.e* , at 532 nm with filled-in beam configuration. The pulse duration is 10 ns. The incident laser beam is split into two vertically polarized beams of equal intensity by the beamsplitter BS_1 with a reflectivity of 10%. The transmitted beam is then split into two beams of equal intensity by the 50% beamsplitter BS_2. The beam transmitted by BS_2 is reflected on to the sample cell SC by a mirror M_1. This beam is the backward-propagating 'read' beam. The beam reflected by BS_2 is in turn reflected onto the sample cell by a mirror M_2. This beam is referred to as forward-going 'pump' or write beam. These two beams are made collinear and counterpropagating by a careful adjustment of the mirrors M_1 and M_2. The reflected beam from BS_1 is further split by a 10% reflecting beamsplitter BS_3 to maintain a high pump–probe ratio. The beam reflected by BS_3 is designated as the forward-propagating 'probe' beam, which is made to interact with the pump beam in the sample cell to form the thermal grating. It is mandatory to satisfy the coherence requirement for the

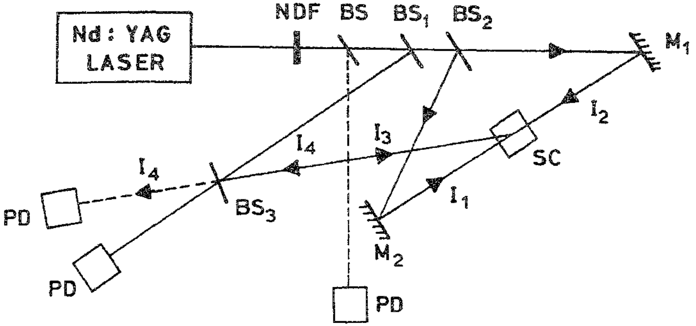

Fig. 1 Experimental layout for OPC–DFWM BS beam splitters, M mirrors, SC:sample cell, PD:photo detector and NDF:neutral density filter

two beams forming the grating by adjusting the path lengths of both the beams. The arrangement is such that the interaction angle could be varied from 10° to about 50°. The absolute beam intensities at various stages in the set-up are measured by pyroelectric and silicon detectors.

For phase conjugation experiments the most essential characteristics of any absorbing medium or dye are strong absorption in the wavelength region of operation, low quantum yields, *i.e.*, low fluorescence so that the excited molecules relax nonradiatively for efficient thermalization and high dissociation energies, and existence of excited state absorption cross section for high-power applications. Based on these properties, metal-substituted tetraphenylporphines with reasonable absorption and low quantum yields are selected. The basic idea behind this choice of nonlinear media is to have a thorough understanding of various properties that contribute to their nonlinearities and to examine the possibility of using them for practical application of phase conjugation.

The absorption and emission spectra of dyes are highly solvent dependent. The solvent dipoles interact with the dipoles of the dye and thus shift the energy levels of the dye. It has been observed that the solvent shift is especially large for dyes whose dipole moments differ appreciably in the ground and excited states. The transition from ground-to-excited state by light absorption is fast compared to the dipolar relaxation of the solvent molecules. Hence the dye molecule finds itself in a nonequilibrium Franck–Condon state following light absorption, and it relaxes to an excited equilibrium state within about 10^{-13} to 10^{-11} s. Similarly, the return to the equilibrium ground state is also *via* a Franck–Condon state, followed by a dipolar relaxation. Therefore, it is clear that in a polar solvent the equilibrium-excited state is lower than the equilibrium ground state by dipole–dipole interaction. The absorption peak usually shifts towards the longer wavelength side with increase in the polarity of the solvent. Investigations have been carried out on four different solvents of varying polarity and their effect on phase conju-

Table I
Figure of merit for different solvents

Solvent	*n*	*[dn/dT](1 exp-5/K)*	$\rho(g/cc)$	$C_p(J/gK)$	$Q^2\ 10^{16}$
Mehanol	1.33118	–36	0.7961	2.51	0.812
Acetone	1.35746	–53	0.792	2.21	2.38
Chloroform	1.446	–55	1.4889	0.9674	4.3
Toluene	1.495	–58	0.8669	1.694	4.92

gate reflectivity. The most important physical parameters of the solvents that have been used for the calculations are presented in Table I.

Porphine systems form the basis for many biological molecules including haemoglobin and chlorophyll. Their conjugated double bond structure and the ability for strong absorption in the visible region of the spectrum causes them to fall within the general classification of organic dyes. The particular class of porphines studied here are the tetraphenylporphines (TPP). The 'electronic' heart of a porphine is the inner 16-membered ring with 18π electrons. The ring is structured with a basic four-fold symmetry, including four nitrogen atoms directed towards the centre. This electronic 'heart' is responsible for the porphine-type optical spectra which are then 'perturbed' to a greater or lesser extent by various chemical modifications to the basic structure.

The structural formula of the free-base tetraphenylporphine(H_2TPP) is given in Fig. 2. Different porphines are formed by substituting the two centre hydrogens with a metal. Considerable difference in electronic and optical properties arise from the central substituent, that is, the atom or group of atoms that occupies the centre of the porphine ring. It is well known from the absorption spectrum studies of porphines that the parent molecule or free base with two hydrogens in the centre has a four-banded visible absorption spectrum distinctly different from the two-banded visible spectrum shown by most metal complexes[11]. It is therefore possible to distinguish a free-base type and metal-

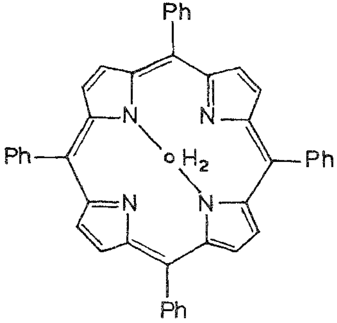

FIG. 2. Structural formula of free-base tetraphenylporphine.

type spectrum. This difference arises from the fact that the two free-base hydrogens in the centre strongly reduce the conjugated ring symmetry from square to rectangular, *i.e.*, from D_{4h} to D_{2h}. The presence of this metal perturbs the π-electron cloud in the porphine ring and this perturbation is dependent on the substituted metal and thus affects its nonlinear properties. TPPs exhibit the phenomenon of reverse saturable absorption, *i.e.*, a decrease in transmission with increasing intensity of incident radiation. This occurs if the absorption cross section from the excited state up to a higher excited state is larger than the absorption cross section of the ground state[12].

Within the class of metalloporphines, it is very well noted that generally there is little change in optical absorption (in some cases strong perturbations are noted in absorption spectra) but substantial change in optical emission properties with a change of metals[13]. Studies of the optical absorption and emission data of the 'Periodic table of the porphines' allow a classification of metalloporphines into two broad classes, *regular* and *irregular*. The regular metals contain only closed shells while the irregular metals contain partly filled shells. The regular porphines include elements of groups I to V, and irregular porphines include elements of groups VII, VIII and IB. In regular porphines the metal has only a small effect on the optical absorption and emission spectra that can be understood as a small perturbation on the π-electrons of the porphine ring. In the case of irregular porphines, the metal orbitals have much stronger effect on absorption and emission, either through stronger mixing with the ring orbitals or through the introduction of new low-energy optical transitions. Because of these qualitative differences between the optical properties of regular and irregular metalloporphines, a systematic study of their nonlinear properties has been taken up with respect to phase conjugation.

4. Results and discussion

In a four-wave mixing geometry, three beams interact to generate the fourth beam which is phase conjugate. As shown in the geometry of FWM (Fig. 1), the probe and pump beams form the grating in the nonlinear medium and the read beam gets diffracted as a phase conjugate beam of the probe. It should be noted that if all three beams are present simultaneously a second transient grating can also be generated by probe and read beams that can contribute to the phase conjugate signal. However, no thermal contribution is obtained from the interaction of the counterpropagating pump and read beams. It is important to understand the role of the angle of interaction and the coherence length of the laser in determining the phase conjugate efficiencies of the nonlinear media. Their characterization can be done only after fixing these two important parameters. It is with this intention that a systematic study of the effects of these two parameters was taken up. Experimentally the dependence of reflectivity on the angle has been verified by increasing the angle between the pump and probe beams, and the result is shown in Fig. 3. It has been found that the efficiency of the system increases with decrease in the angle of interaction. This is due to the fact that with decrease in the interaction angle the interaction volume increases along with the thermal grating decay times. Due to experimental constraints the interaction angle is fixed at 10° for all the investigations that are carried out.

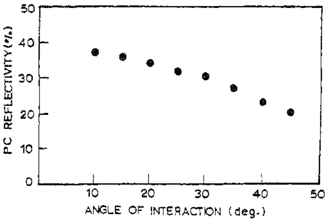

FIG 3 Dependence of phase conjugate reflectivity on interaction angle between pump and probe beams.

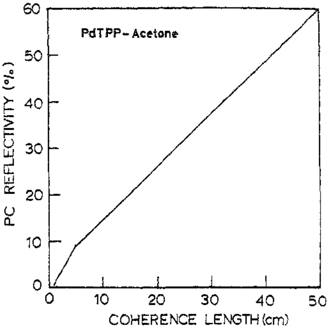

FIG. 4 Dependence of phase conjugate reflectivity on coherence length of the interacting beams

It is well known from the theory of interference that the fringe visibility or the contrast increases with increase in the coherence length of the interfering beams[14]. Physically, this means that the grating formed in the nonlinear media is 'well defined' and 'stationary' so that the diffraction efficiency of the grating is enhanced. Experiments are conducted to study this dependence of phase conjugate efficiency on the coherence time or coherence length (linewidth) of the interacting beams. It is clear from Fig. 4 that phase conjugate reflectivity increases with increase in the coherence length. This implies that the phase conjugate reflectivity is highly dependent on the linewidth of the interacting beams and any meaningful measurements of it should take care of this dependence. In the experiments that are carried out the coherence length of the laser beam is fixed at 50 cm (by fine-tuning the etalon and the electronic line narrower it is possible to increase the coherence length to 500 cm, but it is not possible to fix it at that and single pulse experiments at this coherence length showed further increase in phase conjugate reflectivity as shown in the figure).

For concentration studies, small-angle approximation is made use of and the product of absorption coefficient and interaction length for a given angle θ of 10° between pump and probe beams is fixed at 1.1, *i.e.*, $\alpha L = 1.1$. Here as the interaction length is fixed, the only variable parameter is the absorption coefficient of the TPP. Absorption coefficient is a product of the extinction coefficient and the concentration of the solute. Extinction coefficient is a function of wavelength and it is fixed for a given wavelength of operation (in this case 532 nm), and hence the only variable is the concentration of the solute which determines the absorption coefficient. Absorption spectra for these TPPs in different solvents are taken using a Hitachi 150-20 dual beam spectrophotometer. Phase conjugate reflectivities as a function of concentration in different solvents are measured for an overall incident energy of 50 mJ. The results are discussed separately for regular and irregular TPPs.

As defined earlier, regular porphines include elements of groups I to V whose absorption and emission spectra are essentially determined by the π-electrons of the central substituent. These complexes are generally monometallic, except for the alkali complexes which are bimetallic. This stoichiometric difference does not appear to be significant for the electronic properties[15]. The regular TPPs studied here are H_2TPP, AlTPP, CuTPP, ZnTPP, and VOTPP(vanadium oxide). Their absorption spectra in chloroform and toluene are taken at a concentration of 10^{-5} M/L using a Hitachi dual beam spectrophotometer. The results of concentration effects in regular TPPs are shown in Fig. 5(a). It can be seen from the graph that the peak concentrations are different for different TPPs. The phase conjugate reflectivity increases with increase in atomic weight of the substituted metal.

What is of interest here is the extinction coefficients of these systems at the wavelength of operation for determining their phase conjugate efficiencies. The small differences in the optical spectra of regular TPPs are attributed entirely to $\pi \Rightarrow \pi^*$ transitions of the ring with the central metal contributing only small electronic or spin-orbit perturbations. The electronic perturbations are responsible for the small differences observed among the absorption spectra, while the spin-orbit perturbations cause variations in quantum yields, fluorescence and phosphorescence decay times. Extensive studies have been carried out[16,17] of the emission spectra of TPPs. It is found that heavier the central metal, the lower is their fluorescent quantum efficiency, *i.e.*, the radiationless decay increases with the presence of heavy atoms. The typical fluorescence yields of TPPs range between 0.2 and 10^{-3}, the range being determined by increasing heavy atom effect. The increase in radiationless decay contributes to increase in thermalization which effectively increases the phase conjugate efficiency.

Phase conjugate reflectivities as a function of concentration for irregular TPPs are shown in Fig. 5(b). It can be seen from the figure that the peak concentrations differ for

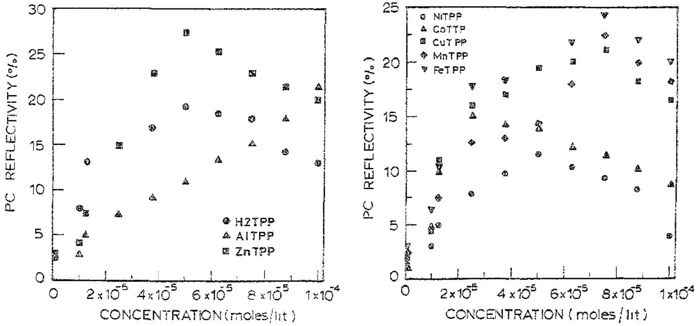

(a) (b)

FIG. 5. Dependence of phase conjugate reflectivity on concentration. (a) Regular, and (b) irregular TPPs

different TPPs and so do the peak phase conjugate reflectivities. The irregular porphines differ from the regular porphines in emission properties and in some cases absorption also. The strong absorption regions for these TPPs are generally blue shifted (hypso) and also in the UV region (hyper). The fluorescent quantum yields are in the region of 10^{-3} to 10^{-6} which imply a strong nonradiative relaxation. Here also the fluorescent quantum yields decrease with an increase in the atomic weight of the substituted metal, *i.e.*, the nonradiative contribution increases with increase in the atomic weight of the substituted metal thus enhancing the phase conjugate reflectivities in that order[17,18].

As discussed earlier, the extinction coefficient is wavelength dependent for any medium. The phase conjugate efficiency in absorbing media has a strong wavelength dependence due to the extinction coefficient for a given concentration of the solute–solvent system. Studying this dependence helps in fixing the wavelength region of operation where maximum efficiency can be achieved. Equation (1) for reflectivity can be rewritten in terms of two factors: one containing the information about the solute–solvent combination, the various timescales involved in the process, the geometrical arrangement and the intensities of the beams while the other pertaining to the explicit and implicit dependence of reflectivity on the wavelength. The expression can be rewritten as[19–21]

$$R = Ae^{-\alpha L \sec\theta} \frac{\left[1 - e^{-\alpha L}\right]^2}{\lambda^2} \tag{9}$$

where

$$A = \frac{4n^2 f^2 (dn/dT)^2}{\rho_0^2 C_p^2} I_1 I_2 G(t_D). \tag{10}$$

While the explicit dependence is λ^{-2}, the implicit dependence of reflectivity of the process on wavelength comes due to the fact that R depends on α which in turn is a function of wavelength and any dispersion effect in the refractive index and (dn/dT).

The experiments are carried out using a pulsed dye-laser (Quanta-Ray, PDL–II), pumped by the second harmonic of Nd:YAG laser. The tunable wavelength range with Rh-6G-methanol system is 550–580 nm. The output power of the dye-laser varies with the wavelength. In the experiments the output of the dye-laser is fixed at 3 MW/cm^2 using calibrated neutral density filters. The experiments are carried out on regular TPPs, and their phase conjugate efficiencies are determined as a function of wavelength. The results are plotted in Fig. 6 and are compared with their absorption spectra. It is very clear from the results that the phase conjugate efficiency is strongly dependent on absorption coefficient of the systems.

The TPPs exhibit the phenomenon of reverse saturable absorption, *i.e.*, their excited state absorption cross section is higher than that of the ground state. Due to this the transmitted intensity decreases with increase in the intensity of the incident radiation and thus the porphines did not show any saturation or bleaching effects within the intensity range of operation. The extinction coefficient for different TPPs is determined as a function of incident intensity. The laser beam is passed through a cuvette containing

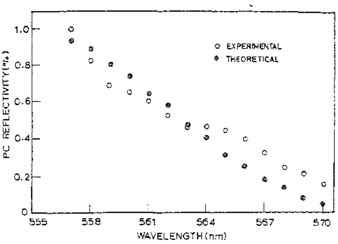

FIG. 6. Wavelength dependence of phase conjugate reflectivity.

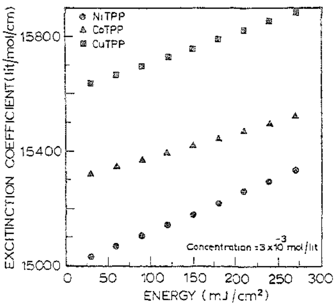

FIG. 7. Variation of extinction coefficients with intensity for different TPPs at 532 nm.

TPP solution of fixed concentration. The incident and transmitted beam intensities are measured using pyroelectric detectors. The extinction coefficients are calculated using Beer's law

$$I = I_0 10^{-\varepsilon c d} \tag{11}$$

where I_0 and I are the incident and transmitted intensities, ε, the extinction coefficient, c, the concentration and d, the distance travelled by the laser beam in the medium. The extinction coefficients for different TPPs in chloroform are shown in Fig. 7. From this figure it is clear that the extinction coefficient increases with intensity or the intensity of the transmitted beam decreases with increase in the intensity of the incident beam. The differences in the extinction coefficients for different systems is due to their absorption characteristics at this wavelength (532 nm). This property of reverse saturable absorption is very useful for high-power applications of phase conjugation.

The variation of the conjugate reflectivity with pump and read beam intensities are studied and the results are shown in Fig. 8. In this experiment the probe beam intensity is kept fixed using calibrated neutral density filters. It can be seen from the graphs that there is a quadratic dependence of conjugate reflectivity on the pump beam intensities. The phase conjugate reflectivity increases linearly with the product of pump and read beam intensities and there is no saturation of phase conjugate efficiency for any of the TPPs, both regular and irregular. This is due to the fact that the TPPs exhibit the phenomenon of reverse saturable absorption.

Equation 2 determines the solvent figure of merit. From the expression for reflectivity it can be seen that it increases with the increase in Q^2 of the solvents. Investigations have been carried out on four different solvents of varying polarity and their effect on phase conjugate reflectivity. The most important physical parameters of the solvents that have been used for the calculations are presented in Table I. Figure 9 compares different solvents for different TPPs for their efficiencies. The important point to be noticed here

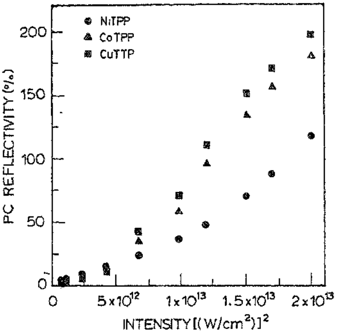

FIG. 8 Intensity dependence of phase conjugate reflectivity for different TPPs

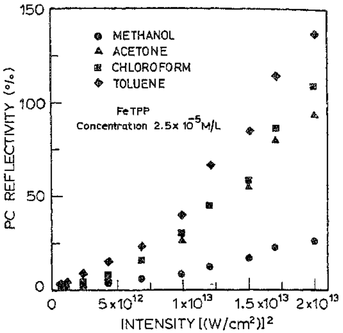

FIG. 9 Comparison of different solvents for their phase conjugate efficiency

is the dependence of phase conjugate efficiency on all the parameters discussed earlier, such as solute and solvent-dependent parameters. The autotracing property of phase conjugation has many potential applications in problems associated with the propagation of high-quality optical beams through distorting media. This property of distortion correction has been observed.

5. Conclusions

The dyes are a class of highly efficient nonlinear media that are compatible with a wide and flexible range of operating conditions. The feature of the thermo-optic interaction that makes it unique in comparison with other nonlinear effects is its adaptability to a variety of different experimental requirements. Thus the nonlinear effect can be tailored for different spectral regions, depending on the availability of dyes with absorption band peaks close to the illumination wavelength and appropriate fluorescent-quenching solvents. The thermal relaxation times and hence the material speed of response can also be varied over a relatively wide range by simply varying the crossing angle θ and choosing suitable solvent parameters. The ready availability of media and the ease with which they can be handled has important practical advantages, especially for high-power applications.

Acknowledgements

The authors gratefully acknowledge late Prof. P. S. Narayanan for his help. This work was carried out with financial support from the Defence Research and Development Organisation (DRDO), Ministry of Defence, Govt. of India.

References

1. Bathra, I. P., Enns, R. H. and Pohl, D. Stimulated thermal scattering of light, *Phys Status Solidi*, 1971, **48**, 11–63.
2. Hoffman, H. J. Thermally induced degenerate four-wave mixing, *IEEE J.*, 1986, **QE-22**, 552–562.
3. Rother, W. Theorie der lichtverstarkung in absorbierenden medien, *Z. Naturforsch. A*, 1970, **25**, 1120–1135.
4. Rother, W., Meyer, H. and Kaiser, W. Amplification of light in absorbing media. stimulated thermal Rayleigh scattering, *Z.Naturforsch. A*, 1970, **25**, 1136–1143.
5. Tocho, I. O., Sibbette, W. and Bradley, D. J. Picosecond phase conjugate reflection from organic dye saturable absorbers, *Opt. Commun.*, 1980, **34**, 122–126.
6. Tocho, I. O., Sibbette, W. and Bradley, D. J. Thermal effects in phase conjugation in saturable absorbers with picosecond pulses, *Opt. Commun.*, 1981, **37**, 67–71.
7. Hoffman, H. J. and Perkins, P. E. Experimental investigations of thermally stimulated degenerate four-wave mixing, *IEEE J.*, 1986, **QE-22**, 563–568.
8. Raghavendra Prasad, B., Krishna Mohan, R., Narayanan, P.S., Subramanian, C. K. and Chandra Sekhar, P. Thermally induced optical phase conjugation by degenerate four-wave mixing, *Curr Sci.*, 1988, **57**, 648–654.
9. Caro, R. G. and Gower, M. C. Phase conjugation by degenerate four-wave mixing in absorbing media, *IEEE J.*, 1982, **QE-18**, 1376–1380.
10. Vijaya, R., Murti, Y. V. J. S., Sundararajan, G., Mathews, C. K. and Vasudeva Rao, P. R. Degenerate four-wave mixing in the cluster C_{60}, *Opt. Commun*, 1992, **94**, 353–356.
11. Dorough, G. D., Miller, J. R. and Huennekaus, F. M. Spectra of the metallo-derivatives of α, β, γ, δ-tetraphenylporphines, *J Am. Chem Soc.*, 1951, **73**, 4315–4320.
12. Blau, W., Byrne, H. and Dennis, W. M. Reverse saturable absorption in tetraphenylporphines, *Opt. Commun.*, 1985, **56**, 25–29.
13. Gouterman, M. Spectra of porphines, *J Mol. Spectrosc*, 1961, **6**, 138–163.
14. Born, M. and Wolf, E. *Principles of optics*, 1989, Pergamon Press.
15. Platt, J. R. *Radiation biology*, (A. Hollaender (ed.)), Vol. 3, Ch. 2, 1956, McGraw-Hill.
16. Seybold, P. G. and Gouterman, M. Porphirenes XIII: Fluorescence spectra and quantum yields, *J. Mol. Spectrosc.*, 1969, **31**, 1–13.
17. Adar, F., Gouterman, M. and Aronowitz, S. Fluorescence, resonance Raman and radiationless decay in several hemoproteins, *J. Phys. Chem.*, 1976, **80**, 2184–2191.
18. Gouterman, M. *Optical spectra and electronic structure of porphines and related rings in the porphines*, Vol. 3 (M. Gouterman (ed.)), 1978, Academic Press.
19. Raghavendra Prasad, B., Krishna Mohan, R., Subramanian, C. K and Narayanan, P. S. Optical phase conjugation studies in metal substituted tetraphenyl porphines, *Proc. Conf. Emerging Optoelectronic Technol.*, Dec.16–20, 1991, pp. 257–260, Indian Institute of Science, Bangalore, India.

20. Krishna Mohan, R., Raghavendra Prasad, B., Subramanian, C. K. and Narayanan, P. S.	Wavelength dependence of phase conjugate reflectivity in absorbing media and thermal grating studies by four-wave mixing, *Pramana*, 1990, **34**, 461–471.
21. Raghavendra Prasad, B.	*Optical phase conjugation studies in molecular gases by stimulated Brillouin scattering and in organic systems by four wave mixing*, Ph. D. Thesis, Department of Physics, Indian Institute of Science, Bangalore 560 012, India, 1993.